Available online at www.scholarsresearchlibrary.com

Scholars Research Library
Archives of Applied Science Research, 2024, 16 (1): 01-15
(http://www.scholarsresearchlibrary.com)

ISSN: 0975-508X

Green Synthesis of Iron (Fe) Nanoparticles Using *Cissus quadrangularis* Stem Extract and Its Role in Photocatalytic Degradation of Methyl Orange

Hemapriya Janarthanam[1*], Reshma Girirajan[1], Rajalakshmi Balaji[1], Jeevitha Prakasam[1], Vijayanand Selvaraj[2]

[1]*Department of Microbiology, DKM College for Women (Autonomous), Vellore, India*

[2]*Department of Biotechnology, Thiruvalluvar University, Serkaddu, Vellore, India*

***Corresponding Author:** Hemapriya Janarthanam, Department of Microbiology, DKM College for Women (Autonomous), Vellore, India*

E-mail: vipni76@gmail.com

***Received:** 26 July, 2023, Manuscript no. AASR-23-110242; **Editor assigned:** 28 July, 2023, Pre QC no. AASR-23-110242 (PQ); **Reviewed:** 11 August, 2023, QC no. AASR-23-110242 (Q); **Revised:** 18 January, 2024, Manuscript no. AASR-23-110242 (R); **Published:** 25 January, 2024*

ABSTRACT

The development of environmentally friendly technologies in the synthesis of materials is of considerable importance for expanding their biological applications. Nanomaterials find many applications due to their behavior at the nanoscale. Among all the methods, biosynthesis of nanomaterials is attracting much attention due to its simplicity, rapidity, no chemical use, non-toxicity and economical approach. Nowadays, many types of inorganic nanoparticles with well-defined chemical composition, size and morphology have been synthesized using different microorganisms and their application in many fields of advanced technology progress has been discovered. Applications of these biosynthesized nanoparticles are in many potential areas including targeted drug delivery, cancer therapy, gene therapy and DNA analysis, antimicrobial agents, biosensors, speed enhancement, separation science, and Magnetic Resonance Imaging (MRI). Nanotechnology has led to more efficient and more precise wastewater treatment methods at both small and large scales. Considering the potential biotechnological applications, this study aimed to synthesize Iron (Fe) nanoparticles from the aqueous extract of Cissus quadrangularis and to characterize the biosynthesized Fe nanoparticles by UV spectroscopy, FTIR, zeta potential, XRD, SEM, EDAX analysis. Furthermore, to probe the photocatalytic degradation of methyl orange by biological Fe nanoparticles under the influence of UV radiation and to evaluate the biodegradation of methyl orange by UV spectroscopy analysis. The experimental design methodology was used to model and optimize the operational parameters of the photocatalytic degradation of methyl orange using Fe nanoparticles by Response Surface Methodology (RSM).

Keywords: Methyl orange, *Cissus quadrangularis*, Fe nanoparticles, Photocatalytic degradation, Response Surface Methodology (RSM)

INTRODUCTION

Nanotechnology is being heralded as a revolutionary technology that has the potential to revolutionize energy efficiency, clean up the environment, and address major health issues. It is claimed to be capable of significantly increasing production output at significantly lower costs. In the near future, nanotechnology may be used to create more efficient power circuits, solar cells, biofuels, and nuclear reactors, as well as to improve the safety of nuclear reactors. Additionally, nanotechnology could lead to significant advancements in healthcare, such as improved methods of diagnosing and treating diseases, such as cancer. Through the synthesis of nanoparticles, nanotechnology has been identified as a potential technology for catalytic converters, industrial processing, and medical applications.

The plant *Cissus quadrangularis*, also known as Veldt Vine, adamant Vine or Devil's backbone, is a member of the grape family and has been used for thousands of years as a natural remedy for a wide range of foods. It has been a part of traditional Indian medical practices since ancient times, including pain relief, menstrual regulation, and fracture treatment. The healing properties of this plant are due to its high vitamin C content and antioxidant compounds such as carotenes, tannins and phenols. Today, extracts from its leaves, roots, and stems are widely available as herbal supplements. They can be found in powder, capsule or syrup form, they are used as a pain reliever and heal broken bones. Indeed, one of its many names is asthisamharaka, which means "thing that prevents bone destruction". *C. quadrangularis* is a plant in the grape family, with red berries and green or yellow flowers. *Cissus quadrangularis* is also the name given to many supplements that claim to support "optimal joint health," "promote healthy bone structure," and support "healthy weight management." There are many claims regarding *C. quadrangularis*, but we can divide them into several different groups, the effects of which are analgesic (pain reliever), anti-inflammatory, antioxidant, complementary bone growth and weight loss. *Cissus quadrangularis* is used for diabetes, obesity, high cholesterol, fractures, allergies, cancer, stomach pain, menstrual pain, asthma, malaria, wound healing, stomach ulcers, weak bones , weak bones (osteoporosis) and as a bodybuilding supplement as an alternative to anabolic steroids. The herb is used for osteoarthritis, rheumatoid arthritis and osteoporosis. Roots and stems are used to treat broken bones. Stem bark boiled with lime water is used to treat asthma. The herb powder is used to treat haemorrhoids and certain bolus infections. The sap is used to treat scurvy, menstrual disorders, nosebleeds and nosebleeds. Grass is fed to cattle to stimulate lactation. Traditionally, the strong, fleshy quadrangular stem has been used to treat acid reflux, gastritis, eye disorders, haemorrhoids, and anemia.

Iron nanoparticles have most promising application in drug delivery. They act as carriers to transport drugs to a specific location. Under the influence of an external magnetic field, the drug containing iron nanoparticles is injected directly into the tumor site. What is also known as a "magnetic drug delivery system"? *Cissus quadrangularis* is a succulent perennial vine widely distributed in warmer regions of India. In English, it is called Edible-stemmed Vine. Based on the morphological features, three different variants have been identified; they are square body, round body and flat body. Common types available are square body and round body. They are rich in ascorbic acid, A-carotene, anabolic steroids and calcium sources. The round-bodied variety is characterized by the presence of a wingless body. The anatomical profile of the stem shows the deposition of characteristic needle or needle-shaped calcium oxalate crystals, raphides and phylogenetic wood in the bundle. The healing properties of *Cissus quadrangularis* have been described as stems, sap, young shoots and total ashes from young shoots were used. The root is useful as a suppository, diaphragm, gastric, emmenagogue and anti-rheumatic. It is useful in the treatment of fractures, dyspepsia, dyspepsia, watery ears, nosebleeds, scurvy, asthma, menstrual irregularities. Indigestion, dyspepsia, diarrhea, fistula can be treated and it is an appetizer. Urinary tract infections, eczema, poison ivy, asthma, obesity, and menstrual disorders are also treated.

An experimental design approach was used to model and optimize the operating parameters of the photocatalytic degradation of methyl orange using Fe nanoparticles. Three experimental parameters were selected as independent variables: pH, initial dye concentration, reaction time. A Central Composite Design (CCD) experimental design was used to establish a quadratic model as a functional relationship between the efficiency of methyl orange decomposition (reactivity) and three independent variables. The degradation efficiency is significantly affected by the initial dye concentration and pH.

MATERIALS AND METHODS

Biogenic approach for the synthesis of Fe nanoparticles

Chemicals used: $FeCl_2$ (99.98%) used as Iron precursor was procured from genuine chemicals, Vellore, India. All the solutions were freshly prepared using double distilled water and kept in the dark to avoid any photochemical reactions. All the glass wares used in experimental procedures were cleaned in a fresh solution of HNO_3/HCl (3:1, v/v), washed thoroughly with double distilled water and dried before use.

Collection of plant materials: Fresh healthy stem of *Cissus quandrigularis* were collected from the market in and around Arni, and Vellore district. The fresh, healthy and mature stem of *Cissus quandrigularis* were used for the present study. Stems were washed thoroughly with running water to remove any dirt or debris on the surface and finally rinsed briefly in deionized water and allowed to shade dry in room temperature.

Preparation of plant extract: The dried *Cissus quandrigularis* stem was grounded and the powder was obtained. 15 grams of *Cissus quandrigularis* stem powder was mixed in 250 ml of distilled water in 500 ml conical flask, then it is kept in the water bath for one hour at 80°C. After cooling, the extract was then filtered through Whatman filter paper no. 1 and stored in a cool and dry place for further work [1].

Phytochemical analysis

The aqueous extract of *Cissus quandrigularis* were tested to detect the presence of various phytocomponents present in the aqueous extract of *Cissus quandrangularis*.

Biosynthesis of Fe nanoparticle using *Cissus quandrigularis*

Iron nanoparticles were synthesized by using the aqueous stem extract of *Cissus quandrigularis*. Equal volume of stem extract (1%) and 0.1 M $FeCl_2$ solution was mixed and incubated in a water bath at 60°C until color change was observed (yellow to mud red). The solution containing iron nanoparticles were separated and concentrated by repeated washing and centrifugation at 10,000 rpm for 15 mins. The final suspension was dried and nanoparticle obtained was used for further experimental studies [2].

Characterization of synthesized Fe_2O_3 nanoparticles

The techniques used for characterization were as follows:

UV–Vis spectral analysis: Synthesis of nanoparticles solution with the culture supernatant of *Cissus quandrigularis* was observed by UV-Vis spectroscopy. The bio reduction of ions in the solution was monitored by periodic sampling of aliquots (1 mL) of the aqueous component after 20 times dilution and measured in the UV-Vis spectra. Samples were monitored as a function of time of reaction using Shimadzu 1601 spectrophotometer in the 100-700 nm range operated at a resolution of 1 nm. The double distilled water used as a blank reference.

Fourier Transform Infra-Red (FTIR) spectroscopy: To remove any free biomass residue or compound that is not the capping ligand of the nanoparticles, after complete reduction, Fe nanoparticles were concentrated by repeated centrifugation (3 times) of the reaction mixture at 15,000 rpm for 20 min. The supernatant was replaced by distilled water each time. Thereafter, the purified suspension was freeze dried to obtain dried powder. Finally, the dried nanoparticles were analyzed by ALPHA FT-IR spectrometer (from Bruker, Germany) for the detection of different functional groups by showing peaks from the region of 4000 cm^{-1} to 500 cm^{-1}.

X-Ray Diffraction (XRD) analysis: The reduced solution was centrifuged at 8000 rpm for 40 min and resulting supernatant was discarded and pellet obtained was re-dispersed in deionized water, centrifuged was repeated three to five times to wash off any adsorbed substances on the surface of the synthesized nanoparticles. Thus obtained purified and dried pellet of synthesis Fe nanoparticles were subjected to X-Ray Diffraction (XRD) analysis.

Scanning Electron Microscopy (SEM) and EDAX: The particle size and morphology of the ferric chloride were examined using scanning electron microscopic observation, SEM measurements were performed on a JEOL JSM 6390 instrument operated at an accelerating voltage at 15 kV. The particle size of the nanoscale materials was measured by nanotract type; ultra-serial number; U2475ES. The sample was sonicated prior to examination for uniform distribution. The composition of the Fe nanoparticles was determined using the EDAX.

Zeta potential and particle size determination (DLS): Dynamic Light Scattering (DLS) and zeta potential of synthesised Fe nanoparticles were analyzed to know the average size and stability of the particles. Nanotrac Wave II, Microtrac Inc, USA analyzer was used to evaluate the crystalline nature and calculate the average size of the particles. For zeta potential analysis the sample was mixed in deionized water and filtered by using 220 nm filter paper.

Determination of antibacterial activity of Fe nanoparticles

Bacterial strains used: Gram negative bacterial strains such as *E. coli*, *Proteus* spp., *Klebsiella* spp., and gram positive bacterial strain *Bacillus* spp., were obtained from the DKMC Laboratory and were used for antimicrobial assay. The selected bacterial strains were inoculated in nutrient broth medium containing beef extract, peptone, sodium chloride and yeast extract at pH 7.0 and then incubated at 37°C. The overnight broth culture was used for investigating the antibacterial activity of Fe_2O_3.

Aqueous extract preparation from *Cissus quandrigularis*

The stem extract of *Cissus quandrigularis* were dried in shade for 1 week and were grinded into fine powder, placed in airtight container at room temperature in the dark. The aqueous extract was prepared by dissolving 10 g of powdered sample in 100 ml of distilled water in a sterile screw-capped 250 ml bottle. The above mentioned arrangement is left undisturbed for 24 h at 4°C. All the sample was filtered using Whatman filter paper no. 2 on a

Buchner funnel.

Agar well diffusion technique

Screening of antibacterial activity was performed by well diffusion technique. The Muller-Hinton agar plates were seeded with 0.1 ml of the standardized inoculums of each test organism. The inoculum was spread evenly over the plate with sterile swab. A standard cork borer of 8 mm diameter was used to cut uniform wells on the surface of the MHA. 100 µl of Fe_2O_3 nanoparticles synthesized from *Cissus quandrigularis* stem extract was added to the well along with standard antibiotics and ferric chloride solution as controls. The inoculated plates were incubated at 37°C for 24 hrs and zone of inhibition was measured.

Application of Fe nanoparticles

Photocatalytic synthetic azo dye degradation potential of (Fe) nanoparticles: Synthetic textile dye used: The commonly used textile dye, methyl orange used in this study was procured. Stock solution was prepared by dissolving 1 g of methyl orange in 100 ml distilled water.

The dye solution was sterilized by membrane filtration (Millipore Millex®-GS, 0.22 mm filter unit), since azo dyes may be unstable to moist-heat sterilization. All the chemicals used in this study were of the highest purity available and of an analytical grade [3].

Photocatalytic degradation assay: To probe the photocatalytic degradation performance of Fe_2O_3 nanoparticles, an aqueous solution of an azo dye, Methyl Orange (MO) was used and the catalytic activity was investigated adding 100 mg of Fe nanoparticles in 100 ml of MO aqueous solution and stirring under the influence of a magnetic stirrer for 30 minutes which would enable the solution to reach equilibrium between the dye molecules and the surface of the nanoparticles.

Besides, the experiment was subjected to colorimeter and the samples were collected at different periods and analysed. The change in dye concentration was analysed through spectroscopy at 450 nm and the percentage of degradation was calculated using the following formula.

$$\text{Decolourization efficiency (\%)} = \frac{\text{Dye(i)} - \text{Dye(r)}}{\text{Dye(i)} \times 100}$$

Where, Dye(i) refers to the initial dye concentration and Dye(r) refers to the residual dye concentration.

Experimental design and optimization by Response Surface Methodology (RSM)

RSM is an efficient technique for the optimization of a multivariable system. In this study, the optimal decolourization efficiency of methyl orange was obtained by RSM using design expert 7.0 [4]. The three independent parameters chosen in this study were the initial dye concentration, pH, and the reaction time. Central Composite Design (CCD), which is the most frequently used form of RSM, was employed to evaluate the influence of the three independent variables [5].

RESULTS

Preparation of plant extract

Fresh healthy stem of *Cissus quandrigularis* was washed thoroughly with running water to remove any dirt or debris on the surface and finally rinsed briefly in deionized water and allowed to shade dry in room temperature (Figures 1 and 2). The dried *Cissus quandrigularis* stem was grounded and the powder was obtained. 15 grams of *Cissus quandrigularis* stem powder was mixed in 250 ml of distilled water in 500 ml conical flask, to obtain the aqueous extract (Figures 3 and 4).

Figure 1. Fresh plant of *C. quadrangularis*.

Figure 2. Dried plant of *C. quadrangularis*.

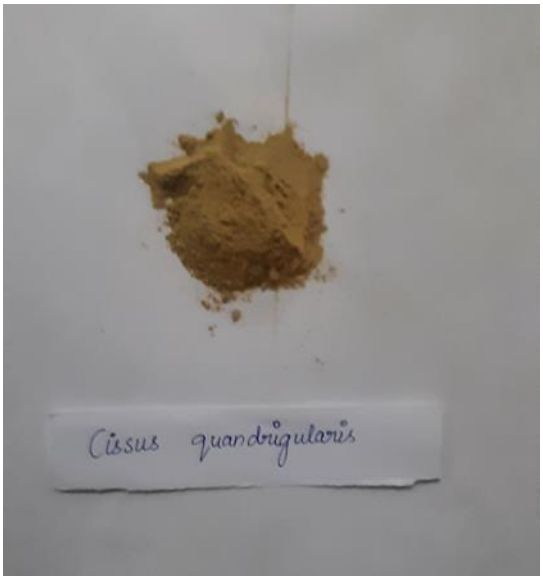

Figure 3. Powdered form of *C. quadrangularis*.

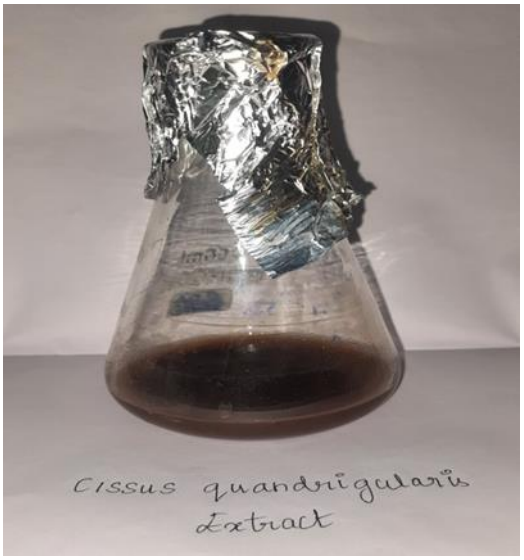

Figure 4. Aqueous extract of *C. quadrangularis.*

Phytochemical analysis of *Cissus quandrigularis*

The phytochemical components of stem extract of *Cissus quandrigularis* was investigated and the results were tabulated in Table 1. The phytochemical analysis revealed the presence of various components such as alkaloids, anthraquinones, flavonoids, saponins, phytosterols, triterpenoids, and poly-phenols (Figure 5).

Table 1. Phytochemical screening of *Cissus quandrigularis* stem extract.

S. no.	Phyto constituents	Result
1	Alkaloids	Negative
2	Carbohydrates	Negative
3	Starch	Negative
4	Reducing sugar	Positive
5	Cardiac glycosides	Negative
6	Protein and amino acid	Negative
7	Flavonoids	Negative
8	Tannin	Negative
9	Phlobatannins	Negative
10	Lignin	Negative
11	Anthraquinones	Negative
12	Anthocyanins	Negative
13	Phytosterols	Positive
14	Saponins	Positive
15	Coumarins	Negative

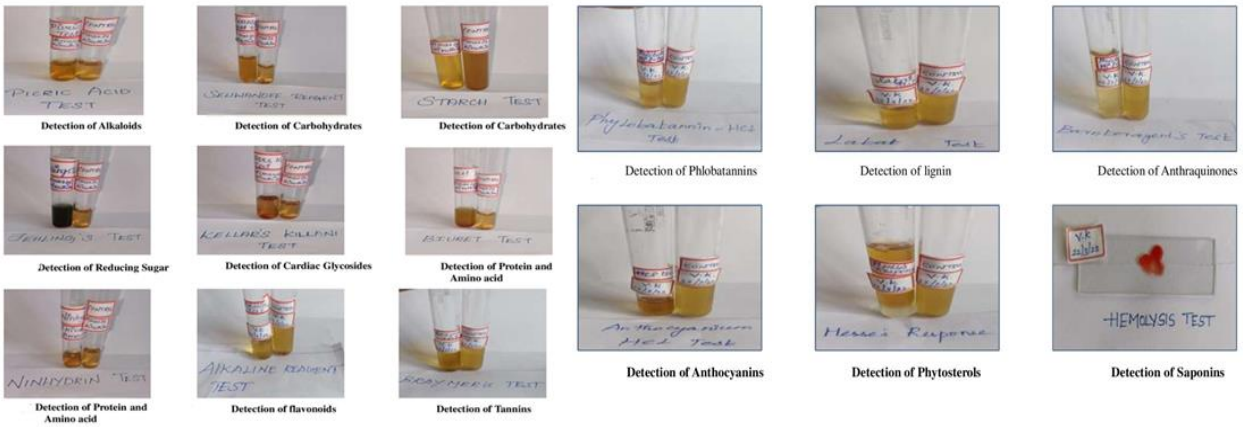

Figure 5. Phytochemical analysis of *C. quadrangularis* stem extract.

Biogenic approach for the synthesis of Fe_2O_3

The biogenic synthesis of Fe_2O_3 nanoparticles using the stem extract of *Cissus quandrigularis* was shown in Figure 6. The color of the solution changed from colorless to mud red indicating the formation of Fe nanoparticles. The solution containing iron nanoparticles was separated, concentrated, and dried. The resultant nanoparticle powder obtained was stored and used for further experimental studies (Figure 6).

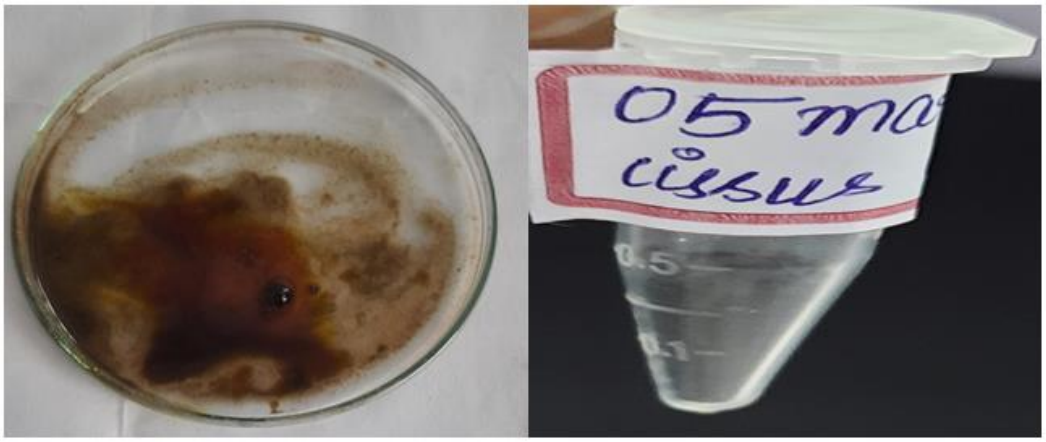

Figure 6. Biosynthesis of Fe nanoparticles (wet and dried form).

Characterization of Fe nanoparticles

UV spectroscopic analysis of Fe nanoparticles

The absorption behaviour arises due to Surface Plasmon Resonance (SPR), which originates from coherent oscillations of electrons in the conduction band of nanoparticles induced by the electromagnetic field therefore spectrometric analysis was considered to be primary tool for characterizing nanoparticles. In our results peak specific for the synthesis of iron nanoparticles was obtained at 200-250 nm by UV Visible spectroscope in the form of a sharp peak (Figure 7).

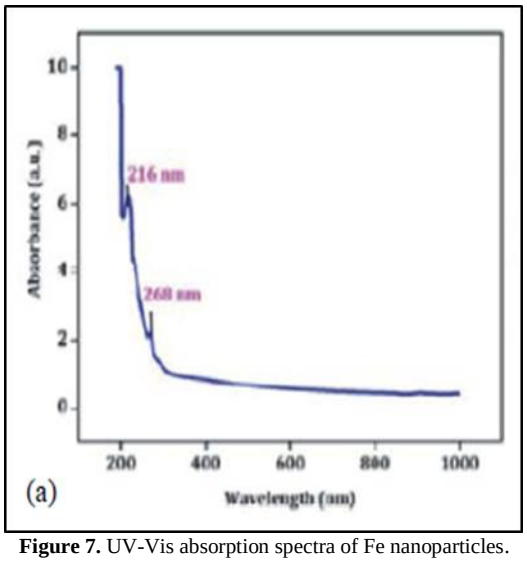

Figure 7. UV-Vis absorption spectra of Fe nanoparticles.

FT-IR analysis of Fe nanoparticles

FTIR spectroscopy is used to probe the chemical composition of the surface and capping agents for the synthesis of NPs. FTIR analysis of synthesized Fe NPs by using the aqueous stem extract of *Cissus quandrigularis* is shown in Figure 8. The synthesized Fe NPs showed the presence of bands due to heterocyclic amine, O-H free bond (3307 cm^{-1}), alkanes, O-H bend (2972 cm^{-1}), C-H, and Carboxylic acid derivative, C-O-H bending (1417 cm^{-1}). The peak at

624.94 clearly ensures the presence of the Fe-O bond in the sample. Hence, the FT-IR analysis of the synthesized sample ensured the synthesis of Fe nanoparticles as well as the existence of various reducing agent functional groups.

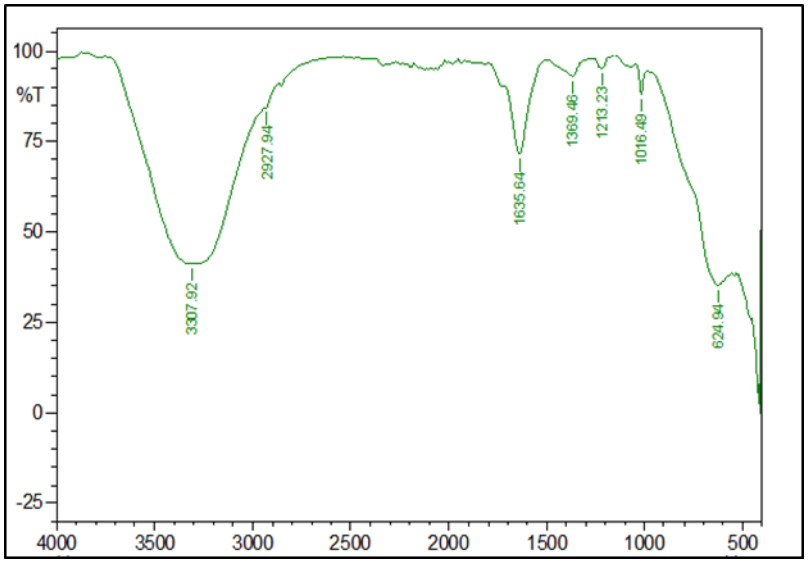

Figure 8: FT-IR spectrum of Fe nanoparticles.

X-ray diffraction analysis of Fe nanoparticles

The XRD data as shown in Figure 9 indicates that the crystal planes of (012), (104), (110), (113), (024), (116) and (018) corresponding to the angles 25.16°, 35.12°, 36.63°, 40.64°, 49.97°, 57.08°, and 59.42° indicates the formation of Fe nanoparticles. The intense and sharp peaks undoubtedly revealed that Fe nanoparticles formed by the reduction method using *Cissus quandrigularis* stem extracts were crystalline in nature.

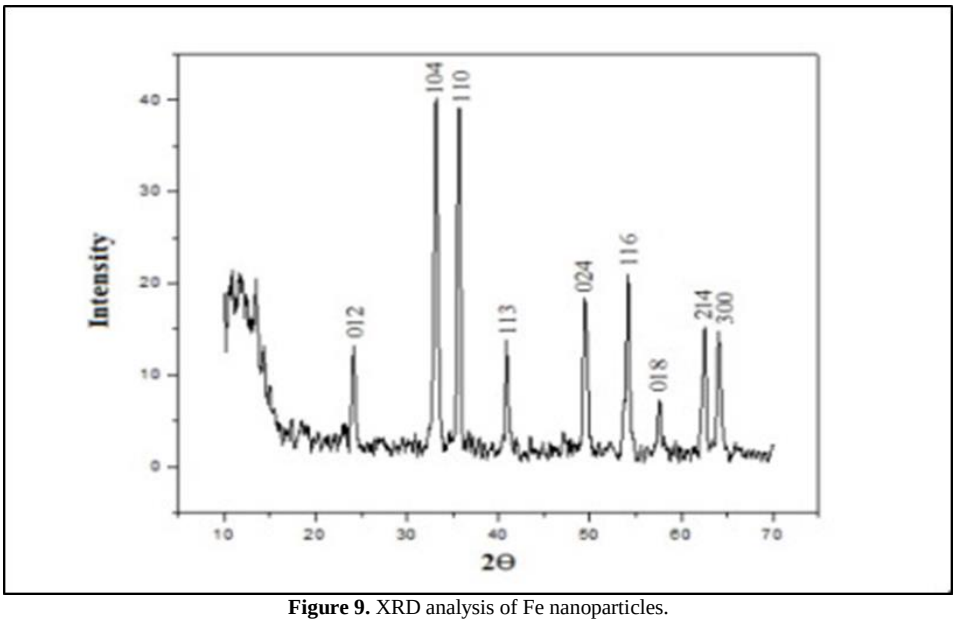

Figure 9. XRD analysis of Fe nanoparticles.

SEM and EDAX analysis

The SEM images of Fe NPs which were obtained from the stem extract of *Cissus quandrigularis* are shown in the Figure 10. The SEM image examines the nature of morphology of the iron oxide nanoparticles and it was found that the particles had pebble like structure and the average size was less than 50 nm with inter-particle distance. Analysis through EDAX confirmed the presence of strong elemental ferric chloride signal of the Fe nanoparticles. The weight percentage of Fe nanoparticles was found to be 43.80% (Figure 11).

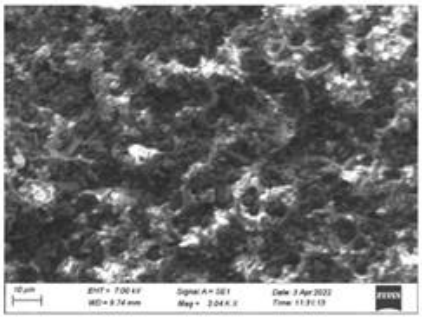

Fig.10 (a) SEM Analysis of Fe Nano Particles

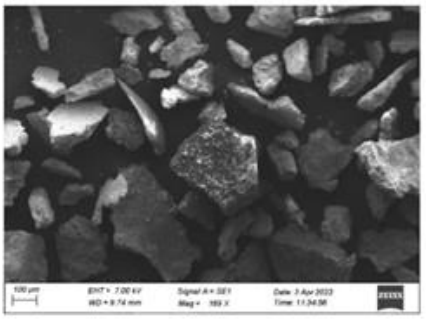

Fig.10 (c) SEM Analysis of Fe Nano Particles

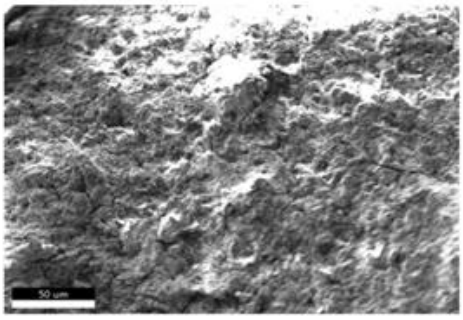

Fig.10 (b) EDAX Analysis of Fe Nano Particles

Figure 10. SEM analysis of Fe nanoparticles.

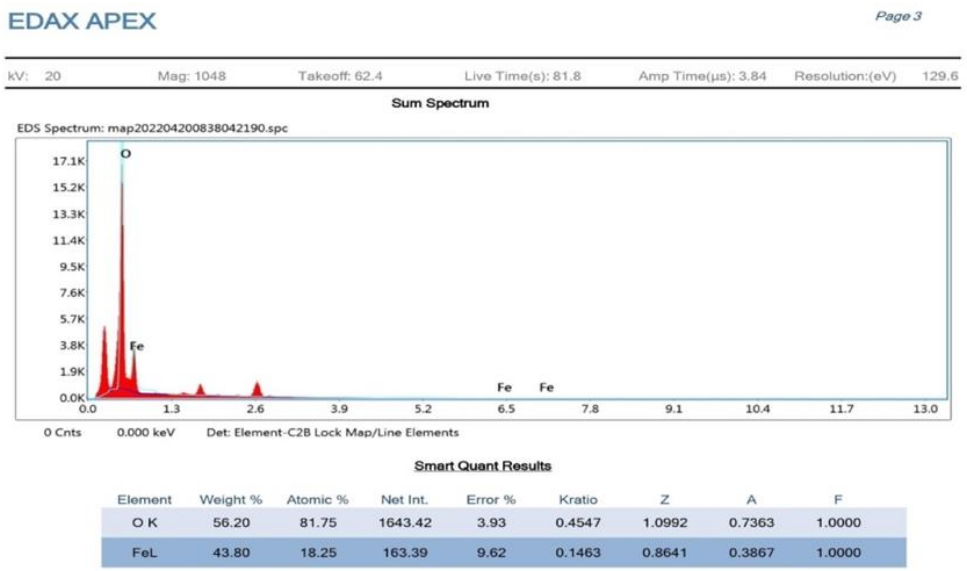

Figure 11. EDAX and electron view of Fe nanoparticles.

Zeta potential and particle size determination (DLS)

Synthesised nanoparticles were dispersed in 10 ml of distilled water to know the particles size with DLS by surpassing laser scattering light and set instrumental conditions like, 0.797 mPa of dispersion medium viscosity, 173° of scattering angle, 25.2°C of temperature. Whereas to know the zeta potential by adding few µl of dispersed nanoparticle solution to electrode and set the conditions like , 622 mS/cm of conductivity, 4.7 V of electrode voltage, 25.2°C of temperature and the data acquisitions time was set to 1 min. Synthesized nanoparticles exhibited polydispersed type of particles with 200 mV of zeta potential value. These outcomes indicated that the plant *Cissus quandrigularis* was a good source for reduction of narrow size of Fe_2O_3 NPs. This indicates synthesized nanoparticles from the stem extract of *Cissus quandrigularis* have higher stability in a liquid medium (Table 2 and Figure 12).

Table 2. Zeta potential analysis of Fe nanoparticles.

Zeta potential (mv)	**200**
Polarity	Negative
Mobility (u/S/V/cm)	15.63
Conductivity (uS/cm)	622
Field strength(kV/m)	4.7

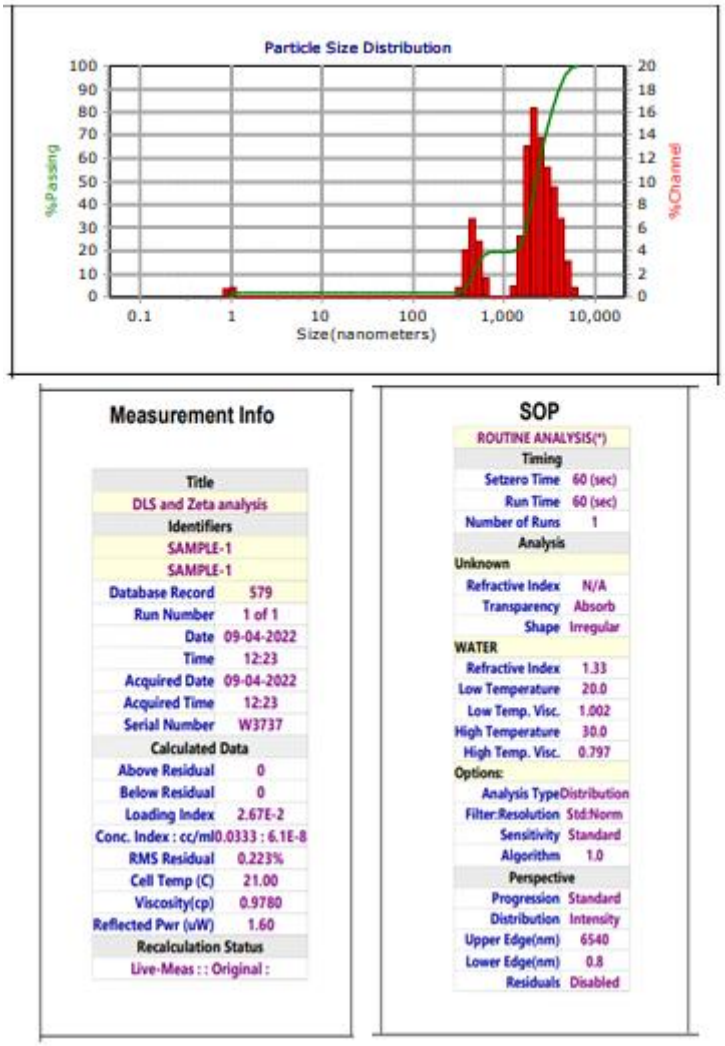

Figure 12. Zeta potential analysis of Fe nanoparticles

Antibacterial activity of iron nanoparticles

Antibacterial activity of biogenic Fe nanoparticles synthesized from stem extract of *Cissus quandrigularis* was investigated comparatively with aqueous plant extract, antibiotic as positive control and Fe solution as negative control (Figure 13). Among the above mentioned, biogenic Fe_2O_3 nanoparticles exerted maximum antagonistic activity than commercial antibiotic against the tested bacterial strains and was followed by aqueous extract which exhibited a very meagre antibacterial activity. Biogenic Fe nanoparticles exhibited significant activity against *E. coli* (25 mm), *Pseudomonas* spp., (20 mm), *Staphylococcus* spp., (20 mm) and *Klebsiella* spp. (20 mm) (Table 3) [6].

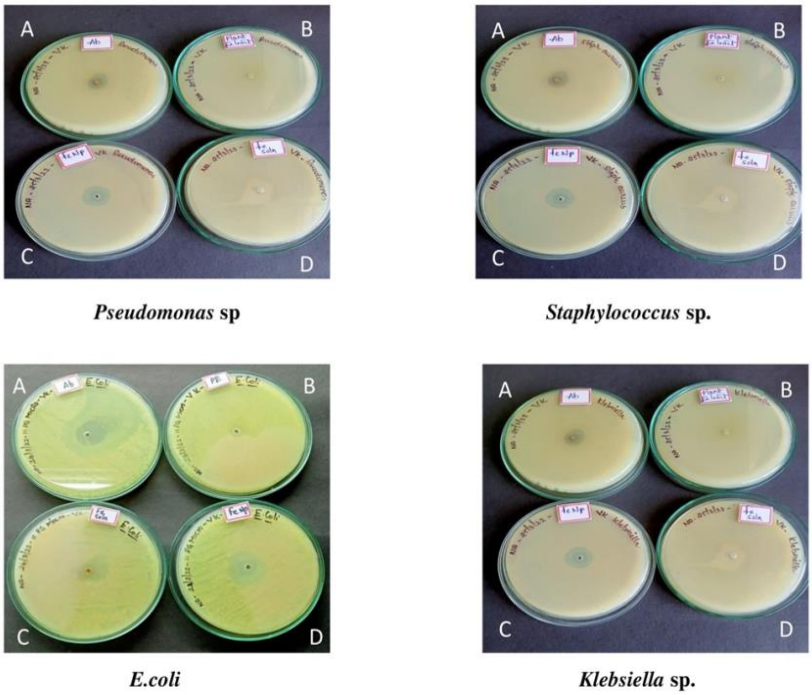

Figure 13. Antibacterial activity of biogenic Fe nanoparticles from *Cissus quandrigularis*. **A:** Positive control; **B:** Plant extract; **C:** Fe NPs; **D:** Negative control

Table 3. Antibacterial activity of Fe nanoparticles.

Bacterial strains tested	Fe NPs	Plant extract	Antibiotic	$FeCl_2$ solution
	Zone of inhibition (mm)			
E. coli	25 mm	3 mm	10 mm	Nil
Klebsiella sp.	20 mm	2 mm	10 mm	Nil
Pseudomonas sp.	20 mm	2 mm	10 mm	Nil
Staphylococcus sp.	20 mm	Nil	10 mm	Nil

Photocatalytic degradation potential of Fe nanoparticles

The photocatalytic degradation of methyl orange (azo dye) dye using Fe_2O_3 nanoparticles synthesized from stem extract of *Cissus quandrigularis* as catalysts was examined (Figure 14). Fe_2O_3 nanoparticles were suspended in Methyl Orange (MO) dye and placed in the magnetic stirrer for 30 mins to acheive adsorption-desorption equilibrium and immediately the photocatalytic degradation experiments were carried out under calorimeter. The graph shows the variation in absorbance of MO dye against irradiation time with Fe_2O_3 nanoparticles.

It is evident that the peak intensity of MO (450 nm) decreases consecutively with time under the exposure of UV light. In our study, after 80 mins, ~90% of MO degradation was observed which was evident by calorimetric analysis at 450 nm and the visual color observation. According to the Beer-Lambert law, absorbance intensity is proportional to the concentration of moieties in solution and our data shows that with increasing time, absorbance of the solution decreases and percentage degradation was increased. When MO dye alone was subjected to photolysis (degradation under calorimeter), no chance in dye concentration was observed.

Similarly, when Fe_2O_3 nanoparticles were subjected in the absence of UV light with the MO solution, only a small change in the concentration of MO was detected as a result of the adsorption of dyes on the surface of nanoparticles. However, when Fe_2O_3 nanoparticles-treated dye was subjected to photocatalysis under calorimeter, substantial dye degradation was observed. These data highlighted the photocatalytic ability of Fe nanoparticles in degradation of methyl orange (Figure 15) [7].

Figure 14. Photocatalytic activity of Fe nanoparticles.

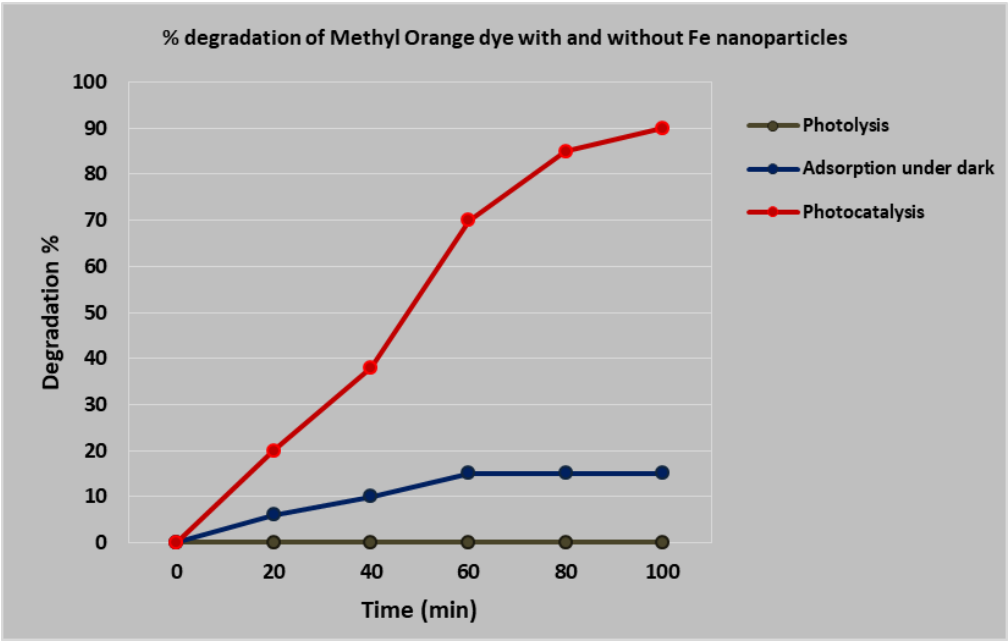

Figure 15. Photocatalytic degradation of methyl orange with and without Fe NPs.

Experimental design and optimization by response surface methodology

Three–dimensional surfaces can be presented as graphical representations to determine the optimal values of the variables and are widely used to achieve better understandings of the interactions between the variables within the range considered. The results of the interactions between three independent variables and the responses are shown in Table 4 and 5 and in Figure 16. Figure 16(a) shows that the dye degradation efficiency decreases with increasing pH value. More information on the interactions between pH value and dye concentration can be obtained from the plots. There is a decrease in degradation efficiency with an increase in pH. Figure 16(b) shows the effects of pH and initial dye concentration. Figure 16(c) shows the effects reaction time and pH of photocatalytic degradation of methyl orange dye [8].

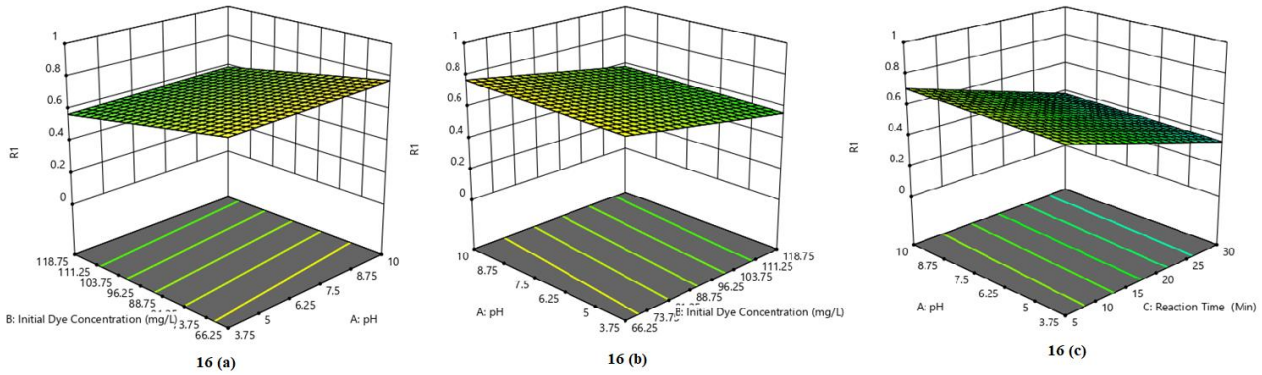

Figure 16. Effect of (a) pH; (b) Initial concentration of dye; (c) Reaction time on photocatalytic degradation of methyl orange

Table 4. Experimental range and levels of independent test variables.

Variables	Range and levels	
	-1	+1
pH	3	10
Initial concentration of dye (mg/L)	66.25	118.75
Reaction time (min)	5	30

Table 5. Experimental design for yield with independent variables, experimental and predicted values of response.

Run	Factor 1	Factor 2	Factor 3	Response 1
	A: pH	B: Initial dye concentration (mg/L)	C: Reaction time (min)	R1
1	6.875	92.5	17.5	0.747454
2	6.875	136.647	17.5	0.178924
3	12.1306	92.5	17.5	0.79578
4	1.6194	92.5	17.5	0.753137
5	3.75	118.75	30	0.451922
6	10	66.25	30	0.598295
7	6.875	92.5	-3.52241	0.901978
8	6.875	48.3529	17.5	0.359519
9	6.875	92.5	17.5	0.257317
10	6.875	92.5	38.5224	0.507052
11	3.75	118.75	5	0.542191
12	10	66.25	5	0.910306
13	6.875	92.5	17.5	0.22297
14	3.75	66.25	5	0.950806
15	3.75	66.25	30	0.329062
16	6.875	92.5	17.5	0.610442
17	10	118.75	30	0.146479
18	6.875	92.5	17.5	0.694237
19	10	118.75	5	0.679517
20	6.875	92.5	17.5	0.219959

DISCUSSION

Biological entities and inorganic materials have been in constant touch with each other ever since inception of life on the earth. Due to this regular interaction, life could sustain on this planet with a well-organized deposit of minerals. Recently scientists become more and more interested in the interaction between inorganic molecules and biological species. Iron nanoparticles were synthesized by using the stem extract of *Cissus quandrigularis*. Fe NPs biosynthesis was confirmed by the change of color from yellow to mud red. Similar observations were made by Pattanayak and Nayak on their studies on *Cissus quandrigularis* stem extracts. The absorption behavior arises due to Surface Plasmon Resonance (SPR), which originates from coherent oscillations of electrons in the conduction band of nanoparticles induced by the electromagnetic field therefore spectrometric analysis was considered to be primary tool for characterizing nanoparticles. In our results peak specific for the synthesis of iron nanoparticles was obtained at 200-250 nm by UV Visible spectroscope in the form of a sharp peak. The SPR phenomenon arises when nanoparticles are

irradiated with visible light, because of the collective oscillations of the conduction electrons [9]. Increasing industrialization and urbanization results in the discharge of waste to the environment, which in turn creates more pollution. The discharge of toxic effluents from various industries adversely affects the water resources, soil fertility, aquatic organisms and ecosystem integrity [10]. The textile industry is one of the greatest generators of liquid effluent pollutants; improper textile dye disposal in aqueous ecosystems leads to the reduction in sunlight penetration and depicts acute toxic effects on aquatic flora and fauna, causing severe environmental problems worldwide. The microbial decolourization and degradation of textile dyes has been of considerable interest since it is inexpensive, eco-friendly and produces a less amount of sludge [11]. Semiconductor heterogeneous photocatalysis is a versatile, low-cost and environmentally benign treatment technology for a host of pollutants. These may be of biological, organic and inorganic in origin within water and air. Heterogeneous photocatalysis has proved to be as an efficient tool for degrading both atmospheric and aquatic organic contaminants.

Heterogeneous photocatalysis uses the sunlight in the presence of a semiconductor photocatalyst to accelerate the remediation of environmental contaminants and destruction of highly toxic molecules. Development of highly robust and solar-light-responsive photocatalysts for the disposal of organic dyes from wastewater is a matter of great significance in order to solve the problems of water pollution. Solar-driven photocatalytic degradation of dyes is considered as a quite efficient, sustainable and cost-effective approach as it involved the inexhaustible and renewable source of energy. In photocatalytic processes, the generation of electron-hole pairs at the surface of the photocatalyst is accomplished by harvesting solar energy. The electron-hole pairs are converted into $^{\bullet}OH$ radicals that are responsible for the degradation of dyes [12].

Incubation time played a substantial role in maximizing the photocatalytic decolorization of methyl orange by iron nanoparticles biosynthesized by using the stem extract of *Cissus quandrigularis*. Dye decolorization efficiency by FeNPs was found to be proportional to the concentration of moieties in solution. Similarly, photocatalytic decolorization of Malachite Green by TiO_2 nanoparticles synthesized by sol-gel method was successfully achieved. Sumitra, et al. reported the photocatalytic degradation of crystal violet within 45 minutes, (C.I. Basic Violet 3) on Nano TiO_2 containing Anatase and Rutile phases (3.1), under UV light by using 125 W high pressure mercury vapor lamp as the source. In contrast, *Citrobacter* spp. CK3 decolorized an azo dye only after 120 h of incubation [13] and Galactomyces geotrichum MTCC 1360 showed optimum decolorization within 18 h of incubation [14].

CONCLUSION

Experimental design methodology was applied to optimize parameters in the photocatalytic degradation of methyl orange using Fe nanoparticles. Heterogeneous photocatalysis has been proved to be an efficient tool for degrading both atmospheric and aquatic organic contaminants. It uses the either UV light or solar irradiation in the presence of a semiconductor photocatalysts to accelerate the remediation of environmental contaminants and destruction of highly toxic molecules. Photocatalysts under either UV light or solar irradiation has become more prominent owing to its low cost, safety, high photocatalytic activity, etc., and as an advanced oxidation technology for the water treatment industry. In addition to the degradation of organic contaminants, the photocatalytic activity of Fe NPs has potential use as an additive in foods or medicines, electrodes of solar cells, etc. a range of nano-microbiological techniques have been proposed or are under active development for treatment of polluted soil and wastewater, but many techniques are still at experimental or pilot stage. In conclusion, there is much recent interest in the exploration of engineered nanomaterial combined with biotechnology *in situ*. In addition, health impacts and environmental fate of these nanomaterials need to be addressed before their widespread application.

Owing to its many advantages mainly involving most stable and active naturally occurring photocatalysts, Fe NPs is, so for, seen as the best catalytic material for degradation of various contaminants and sustainable environmental remediation technology. Therefore, the development of an innovative Fe NPs photocatalysts and its characterization is inevitable to be exploited commercially in photocatalytic water treatment technology. The eco-friendly green chemistry approach for the synthesis of nanoparticles will increase their economic viability and sustainable management. So the exploration of the microbial systems as the potential nanofactories has heightened interest in the biological synthesis of nanoparticles. The “green” route for nanoparticle synthesis is of great interest due to eco-friendliness, economic prospects, feasibility and wide range of applications in nanomedicine, catalysis medicine, nano-optoelectronics, etc. It is a new and emerging area of research in the scientific world, where day-by-day developments is noted in warranting a bright future for this field.

DECLARATION OF COMPETING INTEREST

The authors declare that they have no known competing financial interests or personal relationships that could have appeared to influence the work reported in this paper.

ACKNOWLEDGEMENT

The authors thank PG & Research Department of Microbiology and BENT (Bioprocess Engineering and Nanotechnology) Lab, DKM College for Women (Autonomous), for providing all the necessary equipment and chemicals to carry out this project.

REFERENCES

1. Kanimozhi, S., et al., Biogenic synthesis of silver nanoparticle using *Cissus quadrangularis* extract and its *in vitro* study. *J King Saud Univ Sci*, **2022**. 34(4): 101930.
2. Tien, T. M., et al., Photocatalytic degradation of methyl orange dyes using green synthesized MoS_2/Co_3O_4 nanohybrids. *Catalysts*, **2022**. 12(11): 1474.
3. Vanaja, M., et al., Kinetic study on green synthesis of silver nanoparticles using Coleus aromaticus leaf extract. *Adv Appl Sci Res*, **2013**. 4(3): 50-55.
4. Saien, J., and Mesgari, Z., Photocatalytic degradation of methyl orange using hematoporphyrin/N-doped TiO_2 nanohybrids under visible light: Kinetics and energy consumption. *Appl Organomet Chem*, **2017**. 31(11): e3755.
5. Song, C., et al., Fabrication, characterization and Response Surface Method (RSM) optimization for tetracycline photodegration by $Bi_{3.84}W_{0.16}O_{6.24}$-graphene oxide (BWO-GO). *Sci Rep*, **2016**. 6(1): 37466.
6. Dey, P. C., and Das, R. Enhanced photocatalytic degradation of methyl orange dye on interaction with synthesized ligand free CdS nanocrystals under visible light illumination. *Spectrochim Acta A Mol Biomol Spectrosc*, **2020**. 231: 118122.
7. Shaikh, J. R., and Patil, M., Qualitative tests for preliminary phytochemical screening: An overview. *Int J Chem Stud*, **2020**. 8(2): 603-608.
8. Muthomi, J. W., et al., *In 'vitro'* activity of plant extracts against some important plant pathogenic fungi of tomato. *Aust J Crop Sci*, **2017**. 11(6): 683-689.
9. Anand, R., et al., The i-AAA protease YME1L and OMA1 cleave OPA1 to balance mitochondrial fusion and fission. *J Cell Biol*, **2014**. 204(6): 919-929.
10. Puvaneswari, N., Muthukrishnan, J., and Gunasekaran, P., Toxicity assessment and microbial degradation of azo dyes. *Indian J Exp Biol*, **2006**. 44(8): 618-626.
11. Saratale, R. G., et al., Enhanced decolorization and biodegradation of textile azo dye Scarlet R by using developed microbial consortium-GR. *Bioresour Technol*, **2009**. 100(9): 2493-2500.
12. Vaez, M., Zarringhalam Moghaddam, A., and Alijani, S., Optimization and modeling of photocatalytic degradation of azo dye using a Response Surface Methodology (RSM) based on the central composite design with immobilized titania nanoparticles. *Ind Eng Chem Res*, **2012**. 51(11): 4199-4207.
13. Wang, H., et al., Bacterial decolorization and degradation of the reactive dye Reactive Red 180 by *Citrobacter* sp. CK3. *Int Biodeterior Biodegradation*, **2009**. 63(4): 395-399.
14. Jadhav, S. U., Kalme, S. D., and Govindwar, S. P., Biodegradation of methyl red by *Galactomyces geotrichum* MTCC 1360. *Int Biodeterior Biodegradation*, **2008**. 62(2): 135-142.